Cryogenically Cooled *C*-Band p-i-n Diode Integrated Switch Matrix for Radio Astronomy Applications

GEORGE H. BEHRENS, JR.

Abstract—**A low-loss cryogenically cooled (20 K) eight port *C*-band p-i-n diode switch has been developed for radio astronomy applications. The switching functions are achieved through the use of eight p-i-n diodes in a stripline package. Maximum measured loss and VSWR over the 4.4–5.1-GHz band are 0.75 dB and 1.5:1, respectively. The average measured noise temperature is 9.8 K. The switch provides operational versatility for a dual-channel dual-band (*C*- and *L*-bands) radiometer by simultaneously performing as a Dicke switch, a feed/load selector switch, and a band selector switch. The switch performs these functions at a noise temperature unobtainable with commercially available switches.**

I. Introduction

TO REDUCE the adverse effects of gain instabilities and improve the operational versatility of low-noise radio astronomy receivers, it is usually necessary to incorporate a number of switches ahead of the low-noise preamplifiers. In the past most switched-type radiometers used separate switches to provide the Dicke switching, feed/load selection, and band selection functions. However, with the advent of extremely low-noise cryogenically cooled amplifiers, the noise contribution of such switches can have a significant effect on the overall sensitivity of the radiometer unless steps are taken to reduce the noise temperature of the switches.

In theory, the cooling of such switches can significantly reduce their noise temperatures. Unfortunately, when several switches are involved, the additional space requirements and associated thermal mass can severely hamper the physical arrangement of the Dewar components and increase the cool-down time. Because of these problems, in the design of a new low-noise dual-band (25/6-cm) dual-channel cryogenic receiver [1] at the National Radio Astronomy Observatory, Green Bank, WV, it was decided that a single-multiport coolable p-i-n diode switch be designed which could provide the Dicke switching, feed/load selection, and band selection functions for both receiver channels. Integration of all switching functions in one package also eliminates the necessity of interconnecting cables and connectors between switches and, hence, their attendant loss, and reliability problems.

The design goal was to achieve a switch with minimum loss, VSWR, and noise contribution over the frequency band from 4.5–5.1 GHz and provide the above-mentioned switching functions. In this report, after a brief review of radiometer fundamentals, the various switching modes available, principles of operation, operating characteristics and construction details of the switch are discussed. To the author's knowledge, the only other known report involving the use of cryogenically cooled p-i-n diode switches deals with a SPDT switch operating at *L*-band [2].

Manuscript received December 29, 1977; revised April 10, 1978. The National Radio Astronomy Observatory is operated by Associated Universities, Incorporated, under contract with the National Science Foundation.

The author is with the National Radio Astronomy Observatory, P.O. Box 2, Green Bank, WV 24944.

II. Radiometer Fundamentals

A. The Dicke Radiometer

In radio astronomy the signal levels received are of such low levels that the receiver gain instabilities can seriously limit the effective sensitivity of the radiometer. This effect can be minimized by using the Dicke radiometer as shown in Fig. 1(a). The receiver input is continuously switched between the antenna feed horn and a comparison noise source at a frequency high enough so that the gain has no time to change during one cycle [3], [4].

The detected output V_0 of the Dicke radiometer is proportional to the difference between the antenna noise temperature T_A and the noise temperature of the comparison source T_C:

$$V_0 = K(T_A - T_C) \tag{1}$$

and the minimum detectable signal $\Delta T_{\min}$ is given by the following expression [3] if $T_A = T_C$:

$$\Delta T_{\min} = 2(T_R + T_A)\sqrt{\frac{1}{\beta\tau}} \tag{2}$$

where

T_A antenna noise temperature, K,
T_R receiver noise temperature, K,
β predetection bandwidth, Hz,
τ integration time, s.

In practice the comparison noise source is usually either a microwave termination held at a fixed physical temperature or another antenna feed horn. When a cryogenic receiver is used, the termination is normally held at the operating temperature of the refrigerator (e.g., 20 K). Antenna temperatures are usually around 20 K also, so $T_A \approx T_C$. If there is a significant unbalance between T_A and T_C, noise can be injected via a directional coupler into the colder channel to balance the system or the

0018-9480/78/0900-0629$00.75 ©1978 IEEE

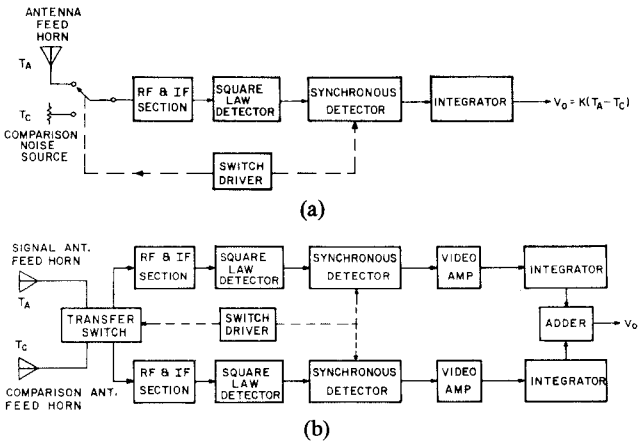

Fig. 1. (a) Single-channel Dicke radiometer. (b) Dual-channel Dicke receiver using the switch beam configuration.

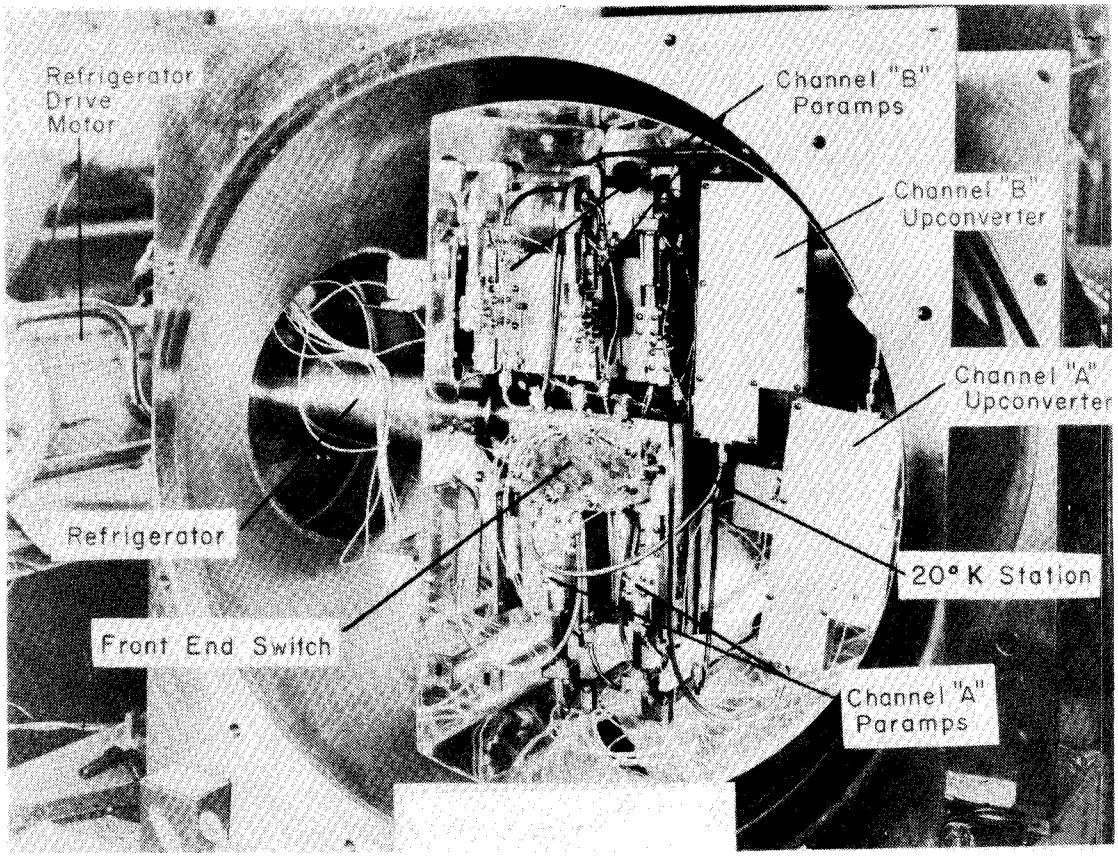

Fig. 2. Front end switch undergoing noise temperature contribution measurements.

receiver gain can be reduced during the higher temperature half of the switch cycle.

When a feed horn is used as the comparison noise source, it is usually identical to the signal feed horn. Both horns are then offset laterally by equal amounts from the focal point of the reflector insuring equal noise temperature for both feeds. This method has the advantage that fluctuations in antenna temperature caused by atmospheric conditions are effectively cancelled since the beams of both feeds see essentially the same area of the atmosphere because their beams are usually only on the order of 2–3 half power beam width apart. However, when observations are made of extended sources, it is advantageous to use the switch load mode of operation; otherwise, both beams will be on source and the output will be distorted. It is, therefore, desirable in the design of a radiometer to incorporate a means to provide both a beam switching mode and a load switching mode.

B. Dual-Channel Operation

In the single-channel Dicke radiometer the signal power is observed only half of the time. However, by switching the signal feed horn between two receivers and adding their outputs as shown in Fig. 1(b), the efficiency of the radiometer is increased. It can be shown that the minimum detectable signal noise temperature of a dual-chan-

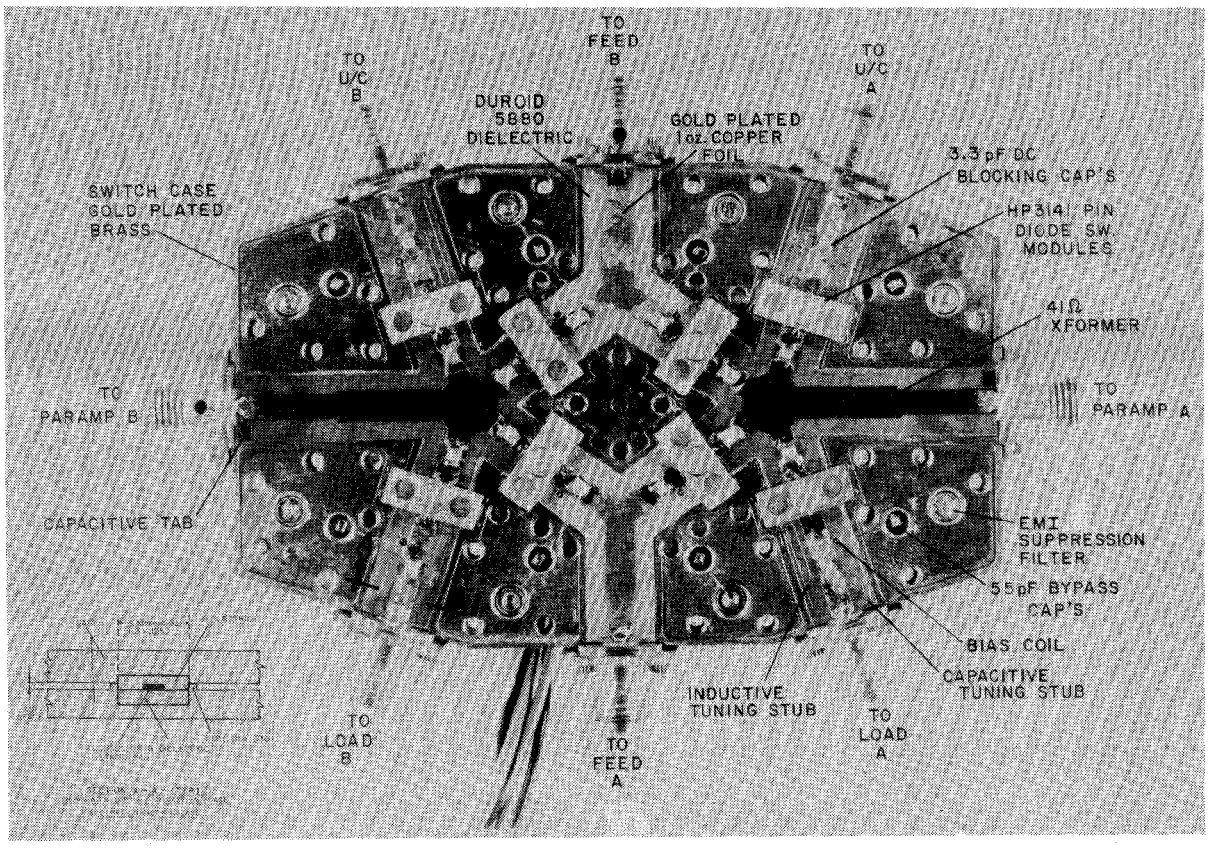

Fig. 3. Front end switch for 25/6-cm receiver.

nel Dicke radiometer is reduced by a factor of $\sqrt{2}$ over a single-channel radiometer [3]. In order to achieve the necessary switch action for a dual-channel Dicke receiver using the beam switching mode, a transfer switch is required.

C. Dicke Switch Design Considerations

One of the major disadvantages of a Dicke radiometer is the increase in receiver noise temperature due to the noise temperature T_{DS} of the Dicke switch. The amount of noise added to the receiver by the loss mechanism of the switch is

$$\Delta T_S = (T_P + T_R)(L-1) \tag{3}$$

and

$$T_{DS} = (L-1)T_P \tag{4}$$

where

- ΔT_S noise added to receiver due to switch,
- T_P physical temperature of switch,
- L loss ratio of switch,
- T_R receiver input noise temperature,
- T_{DS} Dicke switch noise temperature.

Therefore, to minimize ΔT_S, both the physical temperature T_P and the loss L of the switch should be kept to a minimum. In the 25/6-cm radiometer, to minimize T_P the Dicke switch is mounted directly to the 20 K station of the refrigerator as shown in Fig. 2.

In planning the 25/6-cm radiometer, it was decided that a dual-channel Dicke radiometer be implemented. It was also decided that the Dicke switch, besides providing the transfer switching function needed for dual-channel operation, should also incorporate a means to permit either load switching or beam switching for either channel. Further, it was decided that the switch be used to connect the L-band upconverters to the parameteric amplifiers during the 25-cm operation. Dicke switching is not needed during 25-cm operation because only line observations are performed and they are relatively unaffected by gain instabilities.

To satisfy the above requirements, the switch was configured and connected to the radiometer as shown in Figs. 3 and 4, respectively. As shown in Table I there are five different switching modes available. The table shows the connections for the various modes for each half of the switching cycle, e.g., in mode I (both channels load switching), Feed A is connected to Paramp A (2→A) and Feed B is connected to Paramp B (5→B) during the first half switching cycle. During the second half of the switching cycle, loads A and B are connected to Paramps A and B, respectively.

III. Principles of Operation

Referring to Fig. 5, the operation of the switch in the beam switch mode can be explained as follows. Assume RF energy is propagating from Feeds A and B towards junctions J1 and J2, respectively, and diodes D1–D8 are biased as shown during the first half switching cycle.

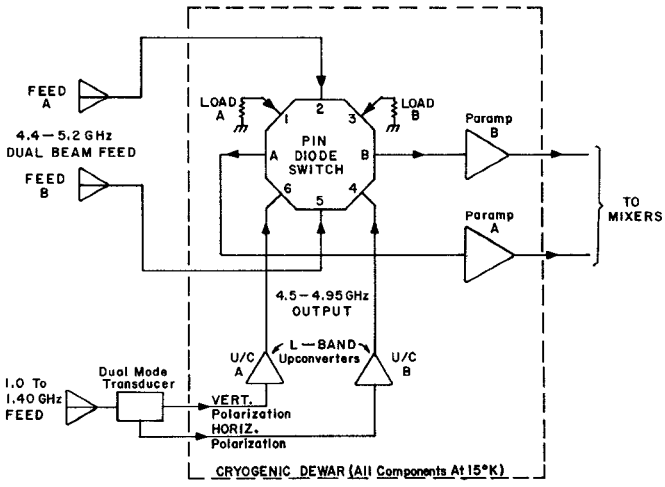

Fig. 4. Block diagram of the front end section of the 25/6-cm cryogenic radiometer.

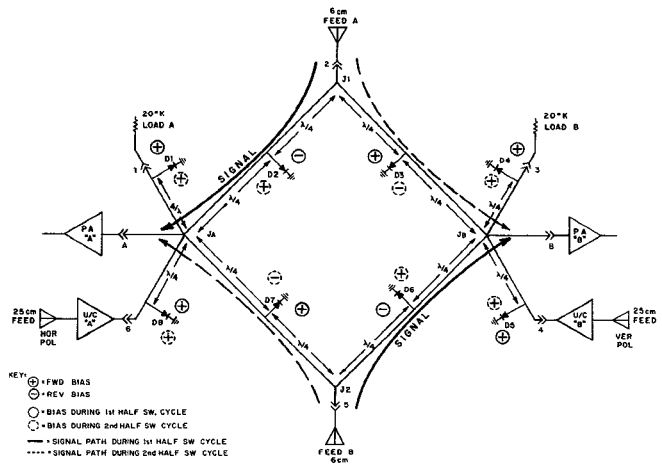

Fig. 5. Simplified schematic of front end switch operating in the beam switching mode.

TABLE I
RF PATHS THROUGH SWITCH FOR VARIOUS SWITCHING MODES

No.	Switching Mode	Connections Made During Switching Cycle	
		First Half Switching Cycle	Second Half Switching Cycle
I.	Both Channels Load Switching	2 → A 5 → B	1 → A 3 → B
II.	Both Channels Beam Switching	2 → A 5 → B	5 → A 2 → B
III.	Channel A Beam Switching Channel B Load Switching	2 → A 5 → B	5 → A 3 → B
IV.	Channel A Load Switching Channel B Beam Switching	2 → A 5 → B	1 → A 2 → B
V.	Both Channels Locked to Upconverters	6 → A 4 → B	No switching.

Next, consider how the energy from Feed A divides at J1 due to the impedance conditions at J1 as seen looking towards JA and JB. Since D3 is forward biased, its low impedance is transformed to a high impedance at J1 by the quarter wavelength 50-Ω transmission line according to the usual quarter wave transformer equation:

$$Z_{IN} = Z_0^2 / Z_d \qquad (5)$$

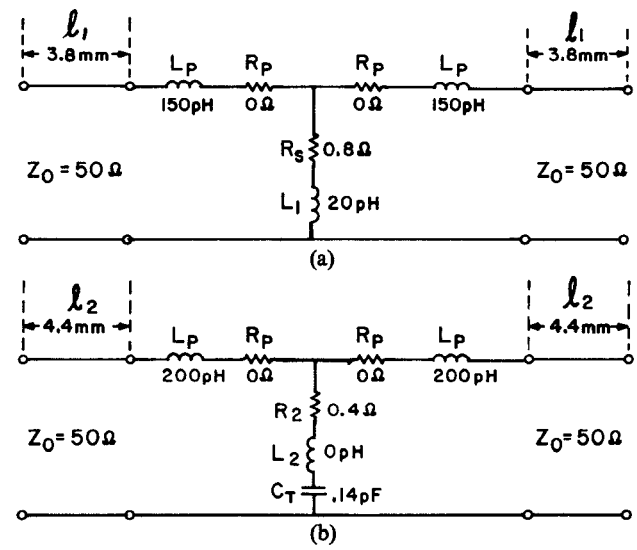

Fig. 6. Room temperature equivalent circuit of the Hewlett-Packard 5082-3141 p-i-n diode.

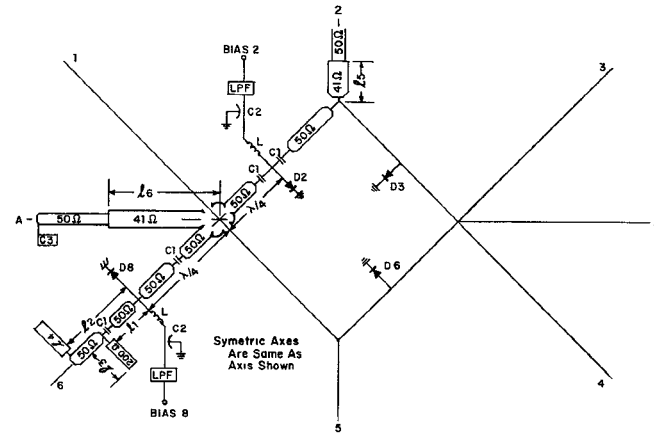

Fig. 7. Diagrammatic layout of switch. Note: All transmission lines are three-layer solid dielectric stripline constructed from 1-oz copper clad duroid 5880.

where Z_0 = characteristic impedance of line and Z_d = forward biased diode impedance. However, the impedance at J1, as seen looking towards JA, is close to 50 Ω since D2 is reverse biased and presents little affect on the line since its impedance is high. Also, diodes D1, D7, and D8 are forward biased causing the impedance looking into each of these arms from JA to be high. Therefore, all the energy entering J1 from Feed A is directed to Paramp P. A. "A" except for the relatively small losses absorbed in the high impedance arms of junctions JA and J1.

The energy arriving at J2 from Feed B can similarly be analyzed to show that it is directed to P.A. "B." During the next half switching cycle the bias conditions of D2, D3, D6, and D7 are reversed causing the RF energy to be directed from Feed A and B to P.A. "B" and "A," respectively. The operation of the switch in the other modes can be explained similarly by referring to Table II which gives the bias conditions for the various switching modes.

The complete schematic of the switch is shown in Fig. 7. Table III gives the values of the various components and the manufacturers' part number.

TABLE II

BIAS CONDITION OF DIODES FOR DIFFERENT SWITCHING MODES

Mode		I		II		III		IV		V	
Half of switch cycle		1st	2nd	1st	2nd	1st	2nd	1st	2nd	1st	2nd
DIODES	D1 ...	FWD	REV	*Fwd*	*Fwd*	*Fwd*	*Fwd*	FWD	REV	*Fwd*	*Fwd*
	D2 ...	REV	FWD	REV	FWD	REV	FWD	REV	FWD	*Fwd*	*Fwd*
	D3 ...	*Fwd*	*Fwd*	FWD	REV	*Fwd*	*Fwd*	FWD	REV	*Fwd*	*Fwd*
	D4 ...	FWD	REV	*Fwd*	*Fwd*	FWD	REV	*Fwd*	*Fwd*	*Fwd*	*Fwd*
	D5 ...	*Fwd*	*Fwd*	*Fwd*	*Fwd*	*Fwd*	*Fwd*	*Fwd*	*Fwd*	*Fwd*	*Fwd*
	D6 ...	REV	FWD	REV	FWD	REV	FWD	REV	FWD	*Fwd*	*Fwd*
	D7 ...	*Fwd*	*Fwd*	FWD	REV	FWD	REV	*Fwd*	*Fwd*	*Fwd*	*Fwd*
	D8 ...	*Fwd*	*Fwd*	*Fwd*	*Fwd*	*Fwd*	*Fwd*	*Fwd*	*Fwd*	*Fwd*	*Fwd*

Capital letters are used to indicate bias condition of diodes switching in that particular mode. Bias conditions of diodes in a fixed bias state are italicized.

TABLE III

COMPONENT DATA

Components	Value	Function	Manufacturer's P/N
C_1	3.3 pF	Blocking capacitor	ATC-100A-3R3-P-50
C_2	56 pF	Bypass capacitor	ATC-100A-560-K-P-50
C_3	0.05" x .075"	Capacitive tap	---
L	---	Bias Injection coil	Piconics 9 1/2 T-47
LPF	---	EMI suppression filter	Erie #1250-003
D1-D8	---	PIN diode	HP 5082-3141
Stripline material	$\varepsilon = 2.23$	---	R/T Duroid 5880
ℓ_1	$Z_0 = 50\ \Omega$ $\ell = .27"$	Transmission line	---
ℓ_2	$Z_0 = 50\ \Omega$ $\ell = .573$	Transmission line	---
ℓ_3	$Z_0 = 200\ \Omega$ $\ell = .700"$	Inductive tuning stub	---
ℓ_4	$Z_0 = 200\ \Omega$ $\ell = 0.195$	Capacitive tuning stub	---
ℓ_5	$Z_0 = 41\ \Omega$ $\ell = .36"$	Impedance transformer	---
ℓ_6	$Z_0 = 41\ \Omega$ $\ell = .55"$	Impedance transformer	---

The 50-Ω transmission line system used is conventional three-layer stripline constructed from photographically etched, copper clad, 0.0625-in thick Teflon/fiberglass. The ground planes are formed by the gold-plated brass case (see Fig. 3): Channels 0.300 in wide and 0.062 in deep were milled in the switch case to accommodate the stripline material. This type of construction was used to maximize isolation between the various arms and achieve good mechanical stability. The ground plane spacing is 0.125 in and the gold plated copper (1 oz) center conductor is 0.100 in wide for $Z_0 = 50\ \Omega$. A small lip was left along the edge of all channels to improve mating surfaces and minimize radiation leakage.

The switching diodes, HP 5082-3141, are silicon p-i-n diodes (see Fig. 6) incased in a 50-Ω hermetic package which permits a continuous transition in the 50-stripline circuit. This stripline package concept, according to Hewlett-Packard [5], "overcomes the limitations in insertion loss, isolation and bandwidth that are imposed by the package parasitics of other discrete devices."

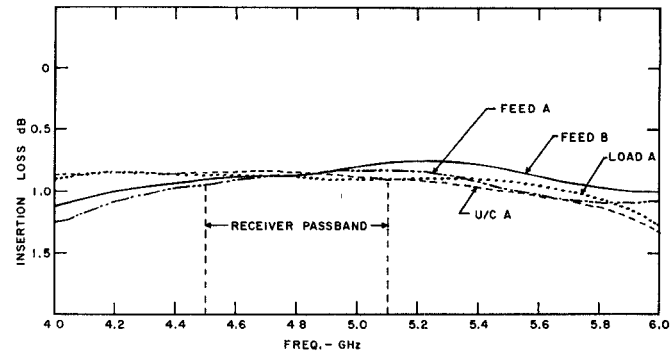

Fig. 8. Insertion loss, paramp "A"→individual ports: $T = 300$ K, $I = 20$ mA/diode.

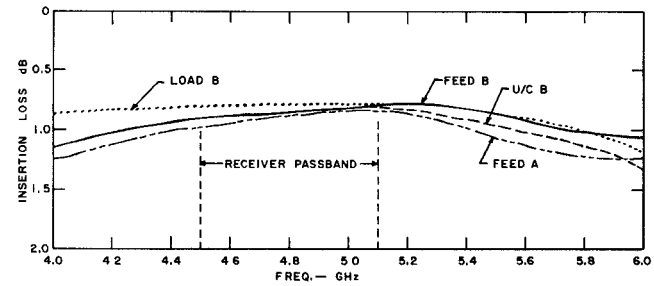

Fig. 9. Insertion loss, paramp "B'→individual ports: $T = 300$ K, $I = 20$ mA/diode.

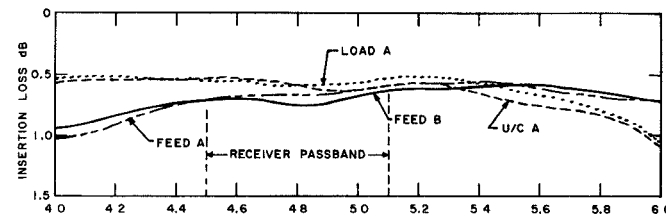

Fig. 10. Insertion loss, paramp "A"→individual ports: $T = 18$ K, $I = 150$ mA/diode.

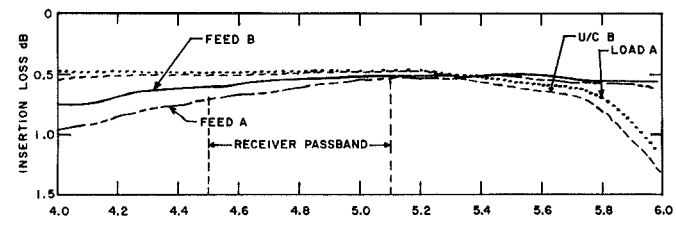

Fig. 11. Insertion loss, paramp "B"→individual ports: $T = 18$ K, $I = 150$ mA/diode.

IV. PERFORMANCE

Measurements were made to determine switch insertion loss, isolation, reflection coefficient, and noise contribution at both 18 K and room temperature conditions. Results of the insertion loss measurements are shown in Figs. 8–11. At 18 K the switch has a maximum loss of 0.75 dB over the operating band of the receiver. Isolation measurements, made in the 4.0–6.0-GHz band, revealed greater than 30-dB isolation between ports. VSWR measurements indicate a maximum VSWR of 1.5 : 1 in the

TABLE IV
MEASURED NOISE CONTRIBUTION DUE TO DICKE SWITCH

	Feed A °K	Feed B °K
Channel A		
Continuum, 4.245-5.040	12.8	14.9
4.6 GHz, 3% bandwidth	10.2	13.3
4.75 GHz, 3% bandwidth	15.2	16.9
4.870 GHz, 3% bandwidth	11.8	13.0
4.920 GHz, 3% bandwidth	13.0	10.0
Average	12.55*	13.5*
Channel B		
4.245 - 5.040	17.4	14.3
4.6 GHz, 3% bandwidth	13.7	9.6
4.75 GHz, 3% bandwidth	18.9	16.76
4.870 GHz, 3% bandwidth	17.8	12.2
4.920 GHz, 3% bandwidth	17.5	14.7
Average	17.0*	13.3*

*Total average. 14.1

Note: A summary of the measured switch characteristics are given in Tables V and VI.

TABLE V
SWITCH CHARACTERISTICS OVER 4.4–5.1-GHz BAND

	Channel A	Channel B
Maximum insertion loss (dB)	0.75	0.75
Maximum noise contribution (°K)	16.9	18.9
Average noise contribution (°K)	13.0	15.2
Maximum VSWR	1.5:1	1.5:1
Minimum isolation (dB)	30	30

TABLE VI
SWITCH CHARACTERISTICS OVER 4.0–6.0-GHz BAND

	Channel A	Channel B
Maximum insertion loss (dB)	1.1	2.0
Noise contribution	Not measured	Not measured
Maximum VSWR	< 2.0:1	< 2.0:1
Minimum isolation (dB)	30	30

passband of the receiver and a maximum of 2.0:1 from 4.0–6.0 GHz. Noise contribution due to the switch was measured at various frequencies across the band by measuring receiver noise temperature with and without the switch connected. The averaged measured noise contribution was 14.1 K. (See Tables IV–VI.) Using (3) and (4), the average switch noise temperature was found to be 9.4 K.

V. DISCUSSION OF RESULTS

Equation (3) can be used to calculate the theoretical noise contribution of the switch ΔT_S. Obviously, however, the accuracy of the calculated value depends very heavily on the accuracy of the values of insertion loss ratio L, receiver noise temperature T_R, and the physical temperature T_P of those components of the switch contributing to the loss. Values of L and T_R can be measured to within ± 2 and ± 10 percent, respectively. with relative ease using standard measurement techniques. However, the value T_P is much more elusive since it is really the effective physical temperature of all the lossy components in the switch (diodes, blocking capacitors, bias coils, and transmission lines) lumped together. Because of this, no attempt was made to make a direct measurement of T_P.

Using the average measured value of receiver noise temperature without the switch ($T_R = 23.2$ K), the measured switch insertion loss of 0.75 dB ($L = 1.19$), and an assumed value of effective physical temperature T_P of 18 K (temperature at which refrigerator was operating), a theoretical value of noise contribution ΔT_S of 7.8 K is obtained from (3). However, the measured value of ΔT_S was 14.1 K or 6.3 K greater than the theoretical value. This difference is thought to be primarily due to the following: 1) impedance mismatch, 2) the assumed value (18 K) for the physical temperature is too low, and 3) inaccuracy in the measured values of L and T_R as mentioned above.

The first effect, impedance mismatch, accounts for only 0.7 K of the 6.3 K difference. This comes about due to the termination on the paramp circulator which can be considered an 18 K noise source. Since the switch has a VSWR of 1.5:1, 0.7 K of the 18 K is reflected at the switch and returned to the paramp as an increase in noise temperature.

The remaining 5.6 K difference is thought to be primarily the result of the measurement inaccuracies of L, T_R, and ΔT_S, and the assumed value of T_P being too low. Measurement inaccuracies can easily account for 2 K with the remaining 3.6 K due to the inaccuracy of the 18 K assumed for T_P. If $T_P = 2.88$ K, this would completely explain the remaining 3.6 K. On the other hand, if we assume no error in the measured values of L, T_R, and ΔT_S, a value of $T_P = 47.3$ K would explain the total 5.6 K difference.

Although no quantitative thermal analysis has been made to determine the theoretical value of T_P, it seems entirely reasonable that its apparent rise from 18 K to some value between 28.8–47.3 K can be attributed to 1) junction heating of the forward biased diodes (150 mA/diode) and 2) the thermal resistance between the lossy components in the switch and the 18 K refrigerator cold station.

VI. CONCLUSION

In the design of radiometers requiring several switches ahead of the cooled preamplifiers, replacing such switches

with a single, cooled, multiport, p-i-n diode switch can provide the following advantages with a minimal noise temperature:

1) elimination of interconnecting cables and connectors between switches and their ensuing loss and reliability difficulties,
2) reduction in space requirements and simplification of system component arrangement, and
3) improved cool-down time due to reduction in thermal mass.

Further improvement in the noise temperature of cooled p-i-n diode switches can probably result from a more judicious selection and impedance matching of the p-i-n diodes. However, information regarding p-i-n diode characteristics at cryogenic temperatures seems to be unavailable, indicating a need for additional work in this area.

ACKNOWLEDGMENT

The author wishes to thank Dr. S. Weinreb of NRAO for suggesting the original switch configuration and T. Wojtowicz, formerly of NRAO, for providing help with the package design. Thanks are also extended to the following employees of NRAO: J. Coe for assisting with the measurements, B. Wright for the excellent machining, A. Miano for preparing the art work and drafting, and C. Dunkle for typing the manuscript.

REFERENCES

[1] J. Coe, "NAIC Receiver," Electronics Division Internal Report No. 180, National Radio Astronomy Observatory, Green Bank, WV, Oct. 1977.
[2] R. Turner, "A low loss coolable switch for Dicke radiometers," thesis University of Virginia, Charlottesville, VA, Aug. 1972.
[3] J. D. Kraus, *Radio Astronomy*. New York: McGraw-Hill, 1966, pp. 248–254.
[4] R. H. Dicke, "The measurements of thermal radiation at microwave frequencies," *Rev. Sci. Instr.*, vol. 17, pp. 268–275, July 1946.
[5] Hewlett–Packard Data Sheet on 5082-3141 PIN diodes.

Subharmonically Pumped Schottky Diode Single Sideband Modulator

JERZY CHRAMIEC

Abstract—**A subharmonically pumped single sideband Schottky diode modulator is described. Its advantages are a large carrier suppression and lowered pumping frequency. The experimental 2-GHz MIC modulator pumped with an 8-mW signal exhibits a conversion loss of 6.2–7.3 dB over a 15-percent frequency band. For a 120-μW input modulating signal, the unwanted components in the output spectrum are at least 18 dB and mostly over 20 dB below the desired sideband.**

I. INTRODUCTION

SEVERAL types of microwave single sideband (SSB) modulators are known. The fundamental method of suppressing one sideband consists in the filtering of the output signal of a double sideband (DSB) modulator. This scheme however has practical limitations for low modulating frequencies and for systems with variable carrier and/or modulating frequency. In such cases balanced SSB modulators may be used, following the principles described in [1] and [2] (Fig. 1). A balanced SSB modulator consists essentially of two DSB modulators and an appropriate dividing, phasing and summing network to suppress one of the sidebands as well as the carrier. Let us consider the conditions of generating a "true suppressed-carrier SSB signal," that is a signal with the carrier and one of the sidebands suppressed for instance by 20 dB with respect to the desired sideband. The sideband suppression factor in this example equals 20 dB and may be attained in either circuit of Fig. 1. The required carrier suppression factor A_p may be evaluated from the formula:

$$A_p[\text{dB}] \geqslant 20 + 10 \log \frac{P_c}{P_m} + L_c \qquad (1)$$

where P_m is the modulating signal power, P_c is the carrier power, and L_c is the modulator conversion loss. Putting $(P_c)/(P_m) \geqslant 25$ (for linear operation), $L_c = 6$ dB, we get $A_p \geqslant 40$ dB. Such a high value of A_p may be obtained only when high-isolation directional couplers as well as perfectly paired and matched diodes are used. The purpose of this paper is to describe a SSB modulator which is

Manuscript received May 26, 1977; revised April 17, 1978.
The author is with University of Basrah, College of Engineering, Electrical Department, Basrah, Iraq.

0018-9480/78/0900-0635$00.75 ©1978 IEEE